JOURNAL OF GEOPHYSICAL RESEARCH, VOL. 90, NO. B12, PAGES 10,291–10,300, OCTOBER 10, 1985

Layered Convection Induced by Phase Transitions

ULRICH R. CHRISTENSEN[1] AND DAVID A. YUEN[2]

Department of Geology, Arizona State University, Tempe

We report a systematic study on the conditions under which an endothermic phase transition can enforce layered convection. Two-dimensional numerical calculations of convection in a domain containing a divariant phase change were performed in the framework of the "extended Boussinesq approximation," i.e., considering the effects of adiabatic gradient, latent heat, and frictional heating in the energy equation. We find that the critical value of the negative Clapeyron slope, which must be surpassed in order to induce layered convection, decreases in magnitude with increasing Rayleigh number Ra in the range $10^4 \leq Ra \leq 2 \times 10^6$. Near the critical Clapeyron slope, vacillations between double- and single-layer convection or strongly leaking double-layer convection are possible. The breakdown into layers is influenced very little by the latent heat release but depends solely on the phase boundary deflection caused by lateral temperature differences. The value of the critical Clapeyron slope also seems little affected by the width of the transition zone or by its depth. A possible superplastic rheology within the transition zone would tend to favor layered convection. Scaling the model results to the 670-km discontinuity in the earth's mantle as a possible endothermic phase boundary, we estimate the critical Clapeyron slope to be in the range of -4 to -8 MPa/K (-40 to -80 bar/K). The possibility that the spinel → perovskite + periclase transition is within this range appears to be remote but certainly cannot be neglected.

1. INTRODUCTION

The nature of the 670-km discontinuity in the earth's mantle is of particular importance in geodynamics because of its possible role of breaking mantle convection into two layers. Traditionally, it has been regarded as a phase change boundary due to the transition of the spinel form of Mg_2SiO_4 into a postspinel structure [*Anderson*, 1967; *Ringwood*, 1972; *Kumazawa et al.*, 1974]. The postspinel form is now identified as a mixture of perovskite ($MgSiO_3$) and periclase (MgO) [*Liu*, 1976]. In the last few years the 670-km discontinuity has also been interpreted as being, at least partially, due to a compositional change [*Anderson*, 1979; *Liu*, 1979]. The question of compositional stratification or uniformity of the mantle is indeed fraught with a great deal of uncertainty [*Jackson*, 1983; *Jeanloz and Thompson*, 1983]. In this work we will treat the density change as one arising purely from a phase transition. Unlike convection with chemical stratifications, for which laboratory experiments can be conducted [*Richter and McKenzie*, 1981; *Olson*, 1984], the dynamics of convection through a phase boundary can only be investigated theoretically or numerically.

It is obvious that a compositionally layered system can remain stable against convective overturn, provided the density difference is large enough. However, an endothermic phase transition has also been suspected of being able to enforce layered convection. A phase boundary interacts with the convective flow in two ways. Where lateral temperature anomalies exist, i.e., in vertical boundary layers, the phase boundary is deflected from its equilibrium position, depending on its Clapeyron slope or pressure-temperature slope $\gamma = dP/dT$. Because of the density contrast Dr between the phases, the deflection is accompanied by buoyancy forces which may help or hinder convection. The other effect is the release of latent heat q_L, which is related to the Clapeyron slope by the Clausius-Clapeyron equation

$$q_L = \gamma \frac{T_a \Delta\rho}{\rho_0^2} \tag{1}$$

where T_a is the absolute temperature and ρ_0 is the mean density. The latent heat may influence the dynamics via thermal expansion and the sensitivity of the phase boundary distortion to temperature. A detailed explanation of these effects can be found in the work of *Schubert et al.* [1975]. The biggest effect is attributed to the phase boundary distortion by the advected temperature [*Olson and Yuen*, 1982], which acts to retard convection when the transition is endothermic (i.e., has a negative Clapeyron slope).

With a time-dependent numerical model containing a "lithospheric slab" (modeled with non-Newtonian temperature-dependent rheology), we were able to demonstrate that double-layer convection occurs with a sufficiently negative γ [*Christensen and Yuen*, 1984]. We determined the critical Clapeyron slope to be -6 MPa/K (-60 bar/K), a somewhat extreme but not outrageous value. In that study we considered only the phase boundary deflection and not the latent heat release, claiming that this is consistent with the Boussinesq approximation commonly used in convection models. Furthermore, our conclusions were based on a single type of model with some arbitrary assumptions (e.g., about slab rheology).

In the present work we start from a set of so-called "extended Boussinesq equations" which include the energy effects of adiabatic compression, latent heat, and frictional heating. In the next section we show that all these three non-Boussinesq effects scale with the same nondimensional parameter (the dissipation number Di) and must therefore be considered or neglected in combination. In contrast to our previous work, we now consider a divariant (gradual) phase change with and without the non-Boussinesq effects. Concerning the rheology, the numerical model is simpler now with essentially constant viscosity, but we are able to cover a wider parameter range than before.

Our main concern is to determine the magnitude of the

[1] Permanently at Max-Planck-Institut für Chemie, Mainz, Federal Republic of Germany.

[2] Now at Department of Geological Sciences, University of Colorado, Boulder.

Paper number 4B5279.
0148-0227/85/004B-5279$05.00

critical Clapeyron slope for the transition to layered convection and its dependence on various parameters. Both time-dependent and steady state finite element results, which address this point, are reported in section 3. We find that breakdown into layered convection occurs more easily the higher the Rayleigh number is. On the other hand, we find no influence of the dissipation number and thus of the latent heat release on the transition point between single- and double-layer convection. Also, we do not find an influence of the depth of the transition, comparing models with equal thickness for both sublayers of convection and models where they break 3 to 7.

An effect of possible importance for the style of convection in the vicinity of a phase boundary is the postulated occurrence of transformational superplasticity while the transition is in progress [*Sammis and Dein*, 1974] or structural superplasticity due to a strong reduction of grain size after the reaction is completed [*Rubie*, 1984]. Both would result in a pronounced reduction of the effective viscosity in or near the transition zone. From models where the viscosity is reduced by a factor of up to 1000 in the transition zone, we conclude that superplasticity has an influence which is moderately favorable for layered convection.

In section 4 we close with a discussion of the geophysical application of our numerical results. Basically, we find our former estimate of -6 MPa/K for the critical γ at the 670-km discontinuity confirmed, although under favorable circumstances the limit might be near -4 MPa/K (-40 bar/K).

2. Constitutive Equations and Numerical Methods

We consider two-dimensional time-dependent convection in a square box with an infinite Prandtl number fluid. Buoyancy forces arise both from density differences due to thermal expansion and from density differences connected with a divariant phase transition. The viscosity η is constant in most models, and in some cases a specific depth dependence is applied, for example, to simulate a low-viscosity zone produced by transformational superplasticity. We fix the temperature contrast ΔT across the layer and take free slip boundaries at the top and bottom and reflective lateral boundaries. The "extended Boussinesq approximation" is applied; that means that except for the driving buoyancy forces the fluid is treated as being incompressible everywhere, including across the phase change region. Additionally, the non-Boussinesq effects of the adiabatic gradient and frictional heating are introduced into the energy equation.

In our formulation we need three equations to solve for the three unknowns, the stream function ψ, the temperature T, and the phase function Γ. Γ describes the relative fraction of the heavier phase and varies between 0 and 1 as a function of pressure p and temperature T [*Richter*, 1973]. We disregard problems which might arise from disequilibrium due to possibly slow reaction kinetics. Contrary to our previous models, where Γ was a step function [*Christensen and Yuen*, 1984], we now take it to be continuous. The transition pressure p_t, i.e., the pressure where $\Gamma = 0.5$, depends on the temperature via the Clapeyron slope γ, where p_0 is the zero-degree transition pressure:

$$p_t = p_0 + \gamma T \qquad \text{(D)} \tag{2}$$

(Equations between dimensional quantities will be marked by a "D" at the end of the equation; nondimensionalized equations do not bear this mark.) We define the "excess pressure" π by

$$\pi = p - p_t = p - p_0 - \gamma T \qquad \text{(D)} \tag{3}$$

and take Γ as a function of π. As *Richter* [1973] discussed, the exact functional dependence is insignificant as long as the transition width d, i.e., the depth range where Γ deviates appreciably from both 0 and 1, is small in comparison with the total height h of the convective layer. Following Richter, we chose a hyperbolic tangent for $\Gamma(\pi)$. To nondimensionalize the equations, spatial quantities are scaled with h, the pressure with $\rho_0 g h$, the temperature with ΔT, and the Clapeyron slope with $\rho_0 g h/\Delta T$, where ρ_0 is the "Boussinesq" density and g is the gravity acceleration. The nondimensionalized Clapeyron slope will be denoted by an overbar $\bar{\gamma}$. The nondimensional vertical coordinate z is taken to be 0 at the bottom and 1 on top of the convection layer. We neglect the nonhydrostatic part of the pressure and obtain the nondimensionalized equations

$$\pi = z_0 - z - \bar{\gamma} T \tag{4}$$

$$\Gamma(\pi) = \frac{1}{2}\left(1 + \tanh \frac{\pi}{d}\right) \tag{5}$$

Because we will make use of this relation later, we also note that

$$d\Gamma/d\pi = \frac{1}{2d}\left(1 - \tanh^2 \frac{\pi}{d}\right) = \frac{2}{d}(\Gamma - \Gamma^2) \tag{6}$$

$d\Gamma/d\pi$ peaks at $\pi = 0$ and becomes negligibly small for $|\pi/d| \gg 1$.

To determine the buoyancy forces in a fluid with a continuous interior phase transition, we take the density to vary according to

$$\rho = \rho_0(1 - \alpha T + \Gamma \Delta\rho/\rho_0) \qquad \text{(D)} \tag{7}$$

where α is the coefficient of thermal expansion and $\Delta\rho$ is the density contrast between both phases. With the Boussinesq approximation this leads to the nondimensionalized momentum equation

$$\nabla^4 \psi = Ra \frac{\partial T}{\partial x} - Rb \frac{\partial \Gamma}{\partial x} \tag{8}$$

where ψ is scaled with the thermal diffusivity κ, Ra is the thermal Rayleigh number

$$Ra = \frac{\alpha g \rho_0 \Delta T h^3}{\kappa \eta} \tag{9}$$

and Rb is the boundary Rayleigh number

$$Rb = \frac{\Delta\rho g h^3}{\kappa \eta} \tag{10}$$

If the viscosity η is nonconstant, the biharmonic operator ∇^4 on the left-hand side of (8) must be replaced by the generalized biharmonic operator [e.g., *Christensen and Yuen*, 1984]. The horizontal variation of Γ is related to the horizontal variation of the temperature

$$\frac{\partial \Gamma}{\partial x} = \frac{d\Gamma}{d\pi}\frac{\partial \pi}{\partial x} = -\bar{\gamma}\frac{d\Gamma}{d\pi}\frac{\partial T}{\partial x} \tag{11}$$

thus (8) can be written as

$$\nabla^4 \psi = Ra\left(1 + \frac{Rb}{Ra}\bar{\gamma}\frac{d\Gamma}{d\pi}\right)\frac{\partial T}{\partial x}$$

$$= Ra\left(1 + P\frac{d\Gamma}{d\pi}\right)\frac{\partial T}{\partial x} \tag{12}$$

where we set for brevity

$$P = \frac{Rb}{Ra}\bar{\gamma} \tag{13}$$

and call P the "phase buoyancy parameter."

The latent heat release per unit volume during the transition is given by

$$Q_L = \rho_0 q_L \frac{D\Gamma}{Dt} \qquad \text{(D)} \tag{14}$$

where $D/Dt = \partial/\partial t + u_i\partial/\partial x_i$ is the material derivative and q_L is the latent heat per unit mass of the complete transition, related to the Clapeyron slope by (1). The extended Boussinesq energy equation [*Oxburgh and Turcotte*, 1978, equation 4.3] is completed by the latent heat term

$$\frac{DT}{Dt} - \frac{\alpha T_a}{\rho_0 c_p}\frac{Dp}{Dt} - \frac{\gamma\Delta\rho T_a}{{\rho_0}^2 c_p}\frac{D\Gamma}{Dt} = \kappa\nabla^2 T + \frac{1}{\rho_0 c_p}\sigma_{ij}\frac{\partial u_i}{\partial x_j} \qquad \text{(D)} \tag{15}$$

where σ_{ij} is the deviatoric stress tensor and u_i are the velocity components. The second term on the left-hand side describes heating by adiabatic compression, and the last term on the right-hand side describes frictional heating. To simplify the equations, the nonhydrostatic pressure is neglected again and nondimensional quantities are introduced. Time is scaled with h^2/κ, velocity with κ/h, and stress with $\eta\kappa/h^2$. A table of the complete nondimensionalization scheme is given by *Christensen* [1984, Table 1]. The non-Boussinesq effects of adiabatic compression and frictional heating depend basically on the dissipation number

$$Di = \alpha g h/c_p \qquad \text{(D)} \tag{16}$$

As an additional parameter of moderate importance, the nondimensional absolute surface temperature T_s enters (scaled with ΔT). It turns out that the nondimensionalization of the latent heat term does not give rise to a new parameter, but the amount of latent heat exchange is governed by a combination of the already defined parameters *Rb*, *Ra*, *Di*, and $\bar{\gamma}$ (nondimensional):

$$\frac{DT}{Dt} + Di\, w\,(T + T_s) - \bar{\gamma}\frac{Rb}{Ra}Di\,(T + T_s)\frac{D\Gamma}{Dt} = \nabla^2 T + \frac{Di}{Ra}\sigma_{ij}\frac{\partial u_i}{\partial x_j} \tag{17}$$

where w is the vertical velocity.

We like to draw attention to the fact that in the classical Boussinesq approximation, which is recovered by setting $Di = 0.0$, the latent heat exchange is neglected. Contrary to the buoyancy effect of the (thermally induced) distortion of the phase boundary, latent heat is a non-Boussinesq effect. We pointed this out in our preceding paper [*Christensen and Yuen*, 1984] as a vindication for ignoring latent heat effects in our models. However, it is not clear if the classical Boussinesq approximation yields good results, especially when rather localized heat sources are neglected, as in the case of phase transitions. On the other hand, if one wishes to take latent heat into consideration, adiabatic and frictional heating must be regarded as well, because they all scale accordingly with the dissipation number. This has not been fully recognized in previous work on phase transitions in convection.

Equation (17) can be rearranged by resolving $D\Gamma/Dt$:

$$\frac{D\Gamma}{Dt} = \frac{d\Gamma}{d\pi}\frac{D\pi}{Dt} = \frac{d\Gamma}{d\pi}\left(\frac{\partial\pi}{\partial T}\frac{DT}{Dt} + \frac{\partial\pi}{\partial z}w\right) = -\frac{d\Gamma}{d\pi}\left(\bar{\gamma}\frac{DT}{Dt} + w\right) \tag{18}$$

which yields

$$\left[1 + \frac{d\Gamma}{d\pi}\bar{\gamma}^2\frac{Rb}{Ra}Di\,(T + T_s)\right]\frac{DT}{Dt} + \left(1 + \bar{\gamma}\frac{Rb}{Ra}\frac{d\Gamma}{d\pi}\right)\cdot(T + T_s)\,Di\,w = \nabla^2 T + \frac{Di}{Ra}\sigma_{ij}\frac{\partial u_i}{\partial x_j} \tag{19}$$

Equation (19) can be interpreted such that in the transition region, where $d\Gamma/d\pi > 0$, the thermal expansion coefficient is altered as

$$\alpha' = \alpha\left(1 + \bar{\gamma}\frac{Rb}{Ra}\frac{d\Gamma}{d\pi}\right) \qquad \text{(D)} \tag{20}$$

and the heat capacity is increased to

$$c_p' = c_p\left[1 + \bar{\gamma}^2\frac{Rb}{Ra}Di\,(T + T_s)\frac{d\Gamma}{d\pi}\right] \qquad \text{(D)} \tag{21}$$

[cf. *Schubert et al.*, 1975].

The effective expansion coefficient α' (equation (20)) is consistent with interpreting the right-hand side of the momentum equation (12) by an effective α'. Note that α' may become negative for an endothermic transition ($\gamma < 0$), whereas c_p' is always larger than c_p.

For fully compressible convection, as treated by *Jarvis and McKenzie* [1980], another nondimensional parameter enters, the compressibility number $K = \alpha g h/K_S = Di/Gr$, where K_S is the (dimensional) adiabatic incompressibility and *Gr* is the Grüneisen parameter. K appears in a now more complicated momentum equation but not in the energy equation. It measures the degree of density stratification. Our extended Boussinesq equations are obtained from the set of fully compressible equations [*Jarvis and McKenzie*, 1980, Table 1] by keeping a nonzero *Di* but setting K to zero or, which is the same, *Gr* to infinity. Since *Gr* is of order 1 for mantle minerals, one might worry how realistic this fluid-dynamical end-member is for the earth. However, Jarvis and McKenzie pointed out that of the three non-Boussinesq effects (adiabatic gradient, frictional heat, and density stratification) the first one has the biggest influence, whereas the density stratification affects only the geometry of the flow. Jarvis and McKenzie did not compare explicitly cases with *Gr* finite and infinite. We reproduced some of their cases, except that in our models $Gr = \infty$. For stationary convection with $Di = 0.25$ (model A3 of Jarvis and McKenzie) there is good quantitative agreement, the differences in the Nusselt number and in the rate of mechanical power generation are 2.5% and 5%, respectively. At $Di = 1.0$, where convection is time dependent, we observe the same principal behavior as that displayed in Figures 13*e* and 13*f* (model C10) of Jarvis and McKenzie: generally two cells and episodic breakup into as many as four cells with a complex flow pattern.

Equations (12) and (19) are solved by a *B* spline finite element technique described elsewhere [*Christensen*, 1984]. We represent ψ by bicubic splines and T by biquadratic splines. We evaluate Γ at each time step according to (4) and (5) in four Gaussian points per element. The additional buoyancy of the distorted phase boundary in (12) is calculated by determin-

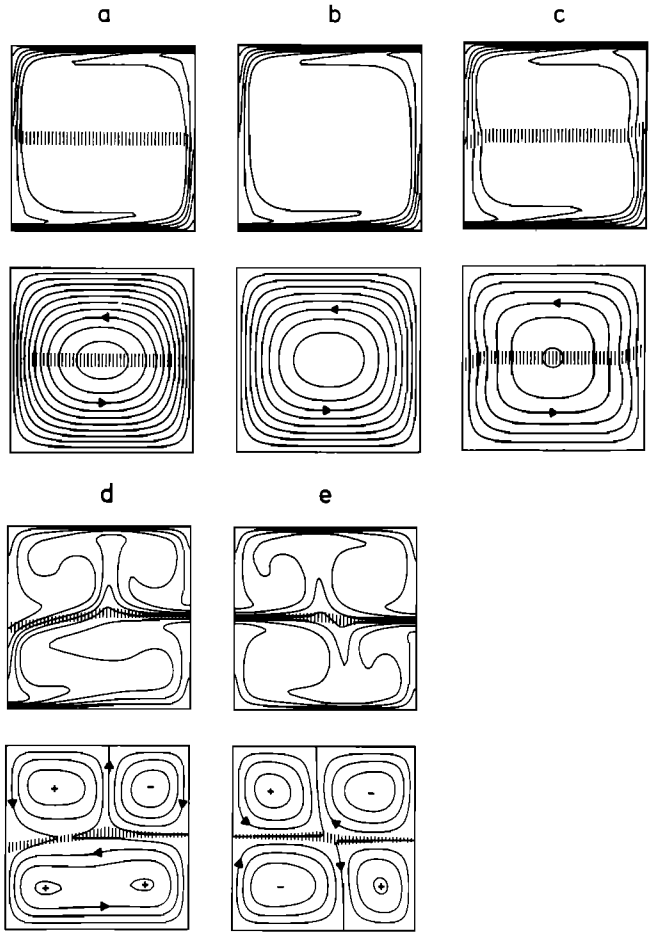

Fig. 1. Isotherms (upper diagrams) and streamlines (lower diagrams) for convection with $Ra = 4 \times 10^5$ and $Di = 0.0$. The phase buoyancy parameter $P = \bar{\gamma}\, Rb/Ra$ is +0.3 in Figure 1*a*, 0.0 in Figure 1*b*, −0.3 in Figure 1*c*, −0.4 in Figure 1*d*, and −0.6 in Figure 1*e*. The region in which $0.2 \leq \Gamma \leq 0.8$ is marked by vertical bars. In Figures 1*a*, 1*b*, and 1*c*, steady state results are displayed, while Figures 1*d* and 1*e* show the situation approximately 2.5×10^{-2} nondimensional time units after the flow was started with a single-layer convection temperature profile. Contour lines for the temperature are 0.05 (+0.10) 0.95 in Figures 1*a*, 1*b*, and 1*c* and 0.10 (+0.10) 0.90 in Figures 1*d* and 1*e*. Isolines for the stream function are drawn every 20 units in Figures 1*a*, 1*b*, and 1*c* and every 8 units in Figures 1*d* and 1*e*.

ing $d\Gamma/d\pi$ from (6) in each Gaussian integration point. The same applies to the modified energy equation (19). The temperature in (19) is calculated implicitly during the time stepping, except for the term $(T + T_s)$, which is taken explicitly, since the numerical equation would become nonlinear otherwise.

The numerical grid is nonuniform with refinement in the horizontal and lateral boundary layers and in the vicinity of the phase boundary as well. It consists typically of 20 to 30 layers of elements in both directions, depending on the Rayleigh number. To ensure the reliability of the method, a number of tests have been performed: (1) convergence tests on refined grids, (2) comparisons with the results obtained with the method of marker chain for a univariant transition with $Di = 0$ [*Christensen and Yuen*, 1984], (3) a comparison for $Di > 0$, but without a phase transition, with results by *Jarvis and McKenzie* [1980], and (4) internal consistency checks. In the first consistency check the amount of the generated mechanical work is compared with the total frictional dissipation, which should be equal:

$$\int (Ra\, wT - Rb\, w\Gamma)\, dV = \int \sigma_{ij} \frac{\partial u_i}{\partial x_j}\, dV \qquad (22)$$

The equality is fulfilled to better than 1%. The second consistency check is to compare the heat flow through the top (Q_{top}) and bottom (Q_{bot}); the difference must be made up by the change of volumetrically stored heat. To determine this last quantity is somewhat complicated because some of the energy is locked up as latent heat which depends intrinsically on the absolute temperature at which the transition takes place. To simplify the calculation, we assume that the average transition temperature is $T_s + 0.5$. The energy balance can then be written in nondimensional units

$$\frac{\partial \langle T \rangle}{\partial t} + \bar{\gamma}\, \frac{Rb}{Ra}\, Di(T_s + 0.5)\, \frac{\partial \langle \Gamma \rangle}{\partial t} \simeq Q_{bot} - Q_{top} \qquad (23)$$

where the angle brackets denote the global average. We find that (23) is fulfilled to within about 2%. Altogether, the generation level of accuracy is estimated to be 1–3%. Even details in the behavior of strongly time-dependent cases appear to be well resolved, as a test with a refined grid on the case depicted in Figure 3 suggests.

3. Results

3.1. *The Boussinesq Limit Di = 0*

In a first series of numerical experiments, the dissipation number is set equal to zero, i.e., the thermal effects of adiabatic compression, frictional heating, and latent heat are neglected.

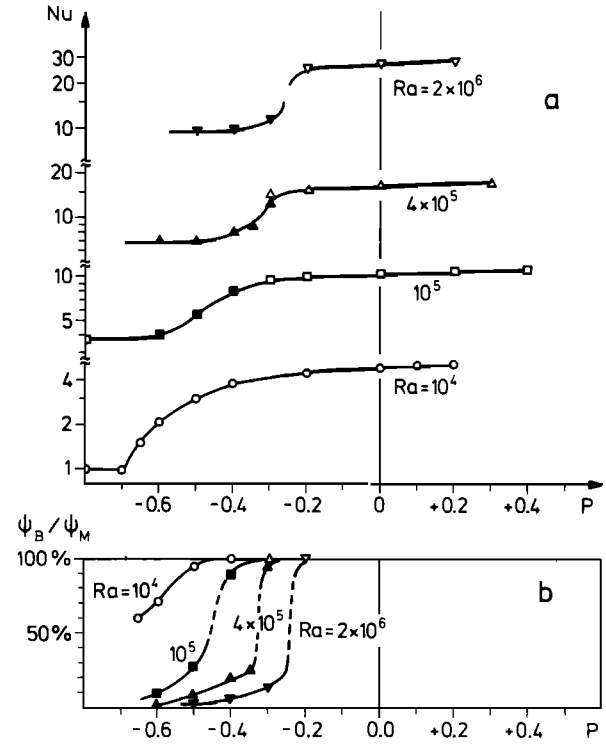

Fig. 2. (*a*) Nusselt number plotted as a function of the phase buoyancy parameter $P = \bar{\gamma}\, Rb/Ra$ for different Rayleigh numbers and $Di = 0.0$. Open symbols are steady state results, while solid symbols give the average from a time-dependent calculation. (*b*) "Rate of leaking" through the phase boundary. The variable ψ_B is the maximum of the stream function on the line where $\Gamma = 0.5$, and ψ_M is the absolute maximum. The meaning of solid and open symbols is as in Figure 2*a*.

To restrict the possible combinations of parameters, Rb has been taken twice as large as Ra in almost all models (i.e., $\Delta\rho/(\rho_0\alpha\Delta T) = 2$), which appears to be representative for phase boundaries in the earth's mantle. A few experiments with different ratios Rb/Ra suggest that the behavior of the system depends mainly on the phase buoyancy parameter $P = \bar{\gamma}\, Rb/Ra$. The half-thickness d of the transition zone (equation (5)) is 0.05 in most models. Experiments with $d = 0.0$ (marker chain), $d = 0.025$, and $d = 0.10$ at $Ra = 10^5$ show very little difference from the standard case, except when the convective system is close to the point of breakdown into layers. Layered convection is slightly more favored by a small d.

Four different Rayleigh numbers of 10^4, 10^5, 4×10^5, and 2×10^6 have been picked, and the equilibrium phase boundary is placed at middepth, i.e., $\Gamma(z = 0.5, T = 0.5) = 0.5$. The Rayleigh numbers for the upper or lower sublayer are 1/16 of the Rayleigh number of the whole layer, provided the temperature contrasts across the sublayers are equal. At positive or mildly negative $\bar{\gamma}$ a successive underrelaxation technique into steady state is applied, which is faster than regular time stepping. For strongly negative $\bar{\gamma}$ or in doubtful cases, the full time-dependent problem is solved. The integration was usually carried out four or five overturn times, when it became obvious that no more qualitative change in the behavior of the system was to be expected, although there was often still a long-term shift in properties like the bottom or surface heat flows. As an initial condition, a conductive boundary layer solution for single-layer convection with small superimposed harmonic disturbances was normally applied:

$$T(x, z, t = 0) = 0.5\left(\operatorname{erfc}\frac{z}{\delta} + \operatorname{erfc}\frac{1-z}{\delta}\right) + A_{11}\cos \pi x \sin \pi z + A_{21}\cos 2\pi x \sin \pi z + A_{12}\cos \pi x \sin 2\pi z + A_{22}\cos 2\pi x \sin 2\pi z \tag{24}$$

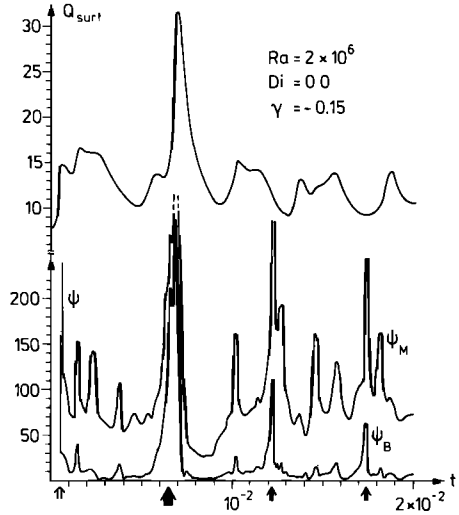

Fig. 3. Evolution of the surface heat flow Q_{surf}, maximum value of the stream function ψ_M, and stream function maximum at the phase boundary ψ_B (equal to the material flux across the boundary) during time, $Ra = 2 \times 10^6$, $Di = 0.0$, $P = -0.30$. The open arrow at the bottom indicates the point where the system breaks down into separately convecting layers (the initial condition corresponding to single-layer convection), the large solid arrow marks the episode of sudden whole layer overturn, and the smaller solid arrows mark the later events of enhanced leaking.

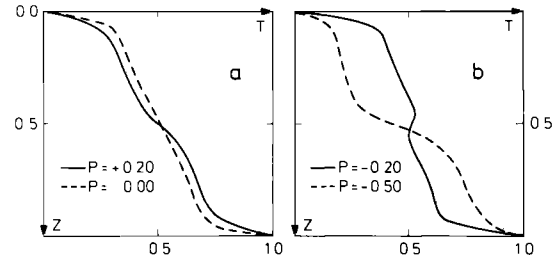

Fig. 4. Horizontally averaged temperature as a function of depth for convection with $Ra = 4 \times 10^5$, $Di = 0.50$, $T_s = 0.50$, and different values of the phase buoyancy parameter P. In case of an exothermic transition ($P > 0$) the adiabatic gradient in the interior of the layer is augmented by a localized increase, in case of an endothermic transition by a decrease in the phase transition zone. When layered convection occurs with strongly negative P (dashed line in Figure 4*b*), thermal conduction in the internal boundary layer dominates the adiabatic and latent heat effect.

with the A_{ij} of the order of 0.01. Tests with different starting conditions, some including an internal thermal boundary layer, suggest that whether or not double-layer convection occurs does not depend on the initial state. However, if double-layer convection occurs, different cell configurations are possible depending on the starting conditions.

At $Ra = 10^4$ the Rayleigh number for each sublayer is below critical ($Ra_s = 625$). At higher Rayleigh numbers, double-layer convection is observed as soon as the phase buoyancy parameter P (or $\bar{\gamma}$) becomes sufficiently negative. Different cell configurations could be realized: two cells of aspect ratio 1 in each layer, two cells in one and a single long cell in the other layer, or one long cell each, which may circulate in a symmetric or antisymmetric mode relative to another. With the most frequently applied initial condition, a configuration of two cells in the upper and one cell in the lower layer was obtained. There are some indications, however, to suggest that a high Rayleigh number and a very negative P, well below the threshold of breakdown, favor two cells in each layer irrespective of the initial condition.

In Figure 1 the effect of decreasing P from mildly positive (Figure 1*a*), to zero (Figure 1*b*), mildly negative (Figure 1*c*), and strongly negative (Figures 1*d* and 1*e*) is displayed. For a moderate P the transition enhances (exothermic) or retards (endothermic) single-layer convection. For sufficiently negative P the original single-layer flow breaks down into two convective layers as soon as the developing vertical boundary layers enter the transition region. Especially in Figure 1*d* it can be seen that the phase boundary is not an impermeable barrier, but a significant fraction of the flow is able to pass through, creating a "leaky" type of double-layer convection [*Christensen and Yuen*, 1984]. In the double-layer regime the actual thickness of the phase transition zone becomes in places much smaller than $2d$ because of the steep temperature gradient in the internal boundary layer.

Figure 2*a* displays the Nusselt number as a function of P for different Rayleigh numbers. In the time-dependent cases the Nusselt number is averaged, starting at some time after the final flow configuration was established. In these cases the accuracy is estimated to be at the 10% level due to the limited integration time, while the steady state results are accurate to about 1%. At $Ra = 10^4$, no double-layer convection is possible, but convection is choked completely for $P \leq -0.7$. In the other cases the transition to double-layer convection is clearly visible as a step in the Nu versus P curve.

As a measure of the mass flux across the phase boundary we

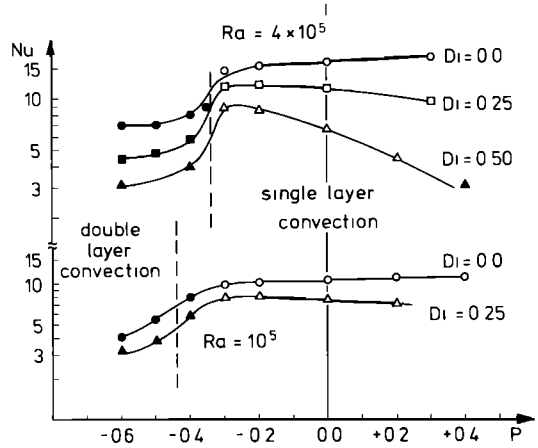

Fig. 5. Comparison of the Nusselt number as a function of P for different values of the dissipation number. Open symbols are from steady state results, and solid symbols are from time-dependent results. In the case $Ra = 4 \times 10^5$, $Di = 0.5$, and $P = +0.4$, two cells of aspect ratio 0.5 (unlayered) emerged.

compare the maximum value of the stream function on the line where $\Gamma = 0.5$ (ψ_B) with the absolute maximum ψ_M. The averaged ratio ψ_B/ψ_M is close to 100% for single-layer convection and below 30% for double-layer convection, decreasing with the (negative) magnitude of P (Figure 2*b*). One important point, which is apparent from Figures 2*a* and 2*b*, is that P needs to be less negative at higher Rayleigh number in order to induce layered convection. The critical phase buoyancy parameter P_{crit}, at which the transition occurs, decreases from about -0.45 at $Ra = 10^5$ to -0.33 at $Ra = 4 \times 10^5$ and to -0.25 at $Ra = 2 \times 10^6$. Over this limited range of Rayleigh numbers the critical P is approximately given by

$$P_{crit} = -4.4\, Ra^{-0.2} \tag{25}$$

An explanation that we can offer for this behavior is that with increasing Rayleigh number, i.e., with decreasing viscosity, the viscous coupling of different parts of the flow becomes weaker. In order to penetrate the transition zone, the localized obstructing buoyancy of the distorted phase boundary must be overcome by the driving buoyancy by thermal expansion, which is distributed over the whole vertical boundary layer. Thus penetration will become less likely the weaker the viscous coupling of different parts of a rising or sinking column is.

The time-dependent behavior at high Rayleigh number near the threshold of breakdown is interesting. At $Ra = 2 \times 10^6$ and $P = -0.30$, layered convection with a leaking rate of typically 10% is established soon after starting the calculation. However, after approximately one overturn of the small cells, the layering broke down temporarily with a heavy mass flux across the phase boundary and a strong increase of the surface heat flow (Figure 3). Approximately one and two overturn times later, short episodes of enhanced leaking are observed, although this time much less dramatic and not accompanied by an increase of surface heat flow. During the first episode of whole layer overturn, approximately 30% of the total material crossed the boundary; during the later episodes of leaking, the fractions are only 5% and 3%, respectively. It is not clear if these episodes are still influenced by the starting conditions and would disappear completely in the long run. However, at $Ra = 10^5$ and $P = -0.4$ an analogous behavior was observed: Most of the time, the flow was in the single-layer regime, but in regular intervals of time the material flux across the boundary became small ($\psi_B/\psi_M \simeq 0.3$) for short periods. This all lends support to speculations that a mixed form of episodic single- and double-layer convection is possible when P is close to its critical value.

3.2. *Finite Dissipation Number*

Calculations with dissipation numbers of 0.25 and 0.50 have been carried out. The latter value may be representative for whole mantle convection. The nondimensional absolute surface temperature T_s has been taken as 0.5, which makes the absolute bottom temperature equal to 1.5 and the average absolute temperature inside the cell approximately equal to 1.0. The choice of $T_s = 0.5$ is intermediate between the values appropriate for convection extending to the surface and convection underneath a lithospheric plate. Steady state solutions with $Di = 0.5$ could only be obtained by heavy numerical damping in the underrelaxation algorithm [cf. *Christensen*, 1984].

In general, a finite Di has an obstructive influence on convection. When the temperature difference between top and bottom is fixed, increasing Di diminishes the potential, i.e., superadiabatic, temperature difference. The latent heat of an exothermic phase transition reduces the potential ΔT further, whereas an endothermic transition increases it. In the examples in Figure 4, with $Di = 0.5$ one half of the temperature difference between top and bottom is made up by the adiabatic gradient, and the potential ΔT is reduced to one half. With $\gamma \neq 0$ the adiabat is modified by an additional localized increase or decrease of temperature in the transition region, which reduces the potential temperature difference to 0.4 ($P = +0.20$) or increases it to 0.6 ($P = -0.20$), respectively. In the single-layer regime, $Di = 0.25$ seems already sufficient to let

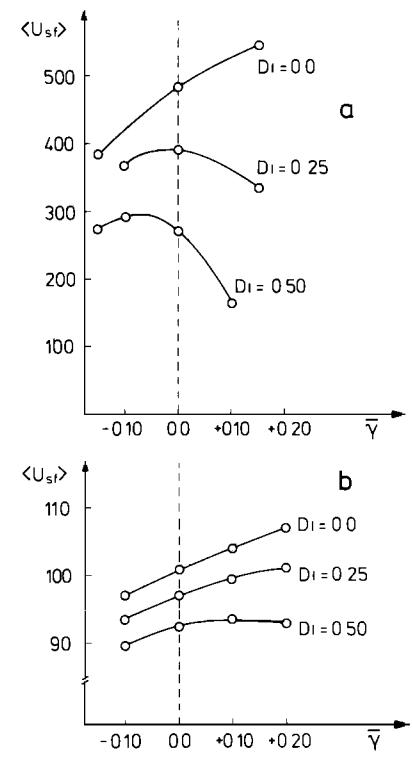

Fig. 6. Average surface velocity as a function of the Clapeyron slope $\bar{\gamma}$. (*a*) The temperature difference from top to bottom is fixed, $Ra = 4 \times 10^5$, $Rb = 8 \times 10^5$, and $T_s = 0.5$. (*b*) The heat flux through the bottom is fixed, and the Rayleigh number based on the heat flow [*McKenzie et al.*, 1974, equation 37] is $Ra^Q = 4 \times 10^5$, $Rb = 4 \times 10^5$, and $T_s = 0.1$.

the latent heat effect dominate the phase boundary distortion effect. With $Di = 0.25$ (and even more so for $Di = 0.50$) a positive P reduces the Nusselt number and a negative P increases it, whereas the tendency is reversed in the Boussinesq case $Di = 0.0$ (Figure 5). This result, that an exothermic transition retards convection when the latent heat influence is considered, is opposite to previous estimates [e.g., *Olson and Yuen*, 1982]. However, to some extent it depends on the applied boundary condition for the temperature. When the heat flux at the bottom is fixed rather than the temperature, the reduction of potential temperature with increasing P will not necessarily apply, but the bottom temperature will simply rise to accommodate the increased adiabatic contribution. In Figure 6 it is demonstrated that the convective motion is much more influenced by the latent heat effect, or finite Di, when the temperature is fixed rather than in the case of fixed heat flux.

Regarding the pronounced effect of latent heat in the single-layer regime, at least for the case of fixed temperature contrast, one might expect that a finite Di would have a strong destabilizing influence on layered convection. However, quite surprisingly, the value of Di has no influence on the critical P, the threshold at which breakdown into two layers of convection occurs. The sudden decrease of the Nusselt number which marks this breakdown is always in the same range, as displayed in Figure 5 for $Ra = 10^5$ and 4×10^5. Also, the leaking ratios (ψ_B/ψ_M) are found to be virtually identical at the same values of Ra and P irrespective of the dissipation number. For $Ra = 2 \times 10^6$, only a single time-dependent run was carried out (with $Di = 0.50$, $P = -0.30$), but this one corroborates the previous conclusion. The time-dependent behavior is very similar to the case with $Di = 0.0$, which was discussed in the preceding section: generally we found double-layer convection, interrupted by a large event where layering was temporarily destroyed and by subsequent smaller events of enhanced leaking. We can only speculate on the reasons why latent heat has no effect on the threshold to layered convection despite its rather strong influence on the convective motion in the single-layer regime. The additional heat affects the buoyancy forces in two ways [cf. *Schubert et al.*, 1975, Figures 1 and 2]. Latent heat combined with ordinary thermal expansivity is indeed destabilizing (i.e., promotes convective motion) for endothermic transitions and stabilizing for exothermic transitions, which explains the observed behavior in the single-layer regime. However, the mechanism for convective layering depends more on local processes in the vicinity of the phase boundary. In this respect, the response of the phase boundary distortion to the release of latent heat becomes important, and this effect is stabilizing (retards convective motion), regardless of the sign of γ. Possibly, the two effects just cancel approximately, as far as the mechanism for stabilizing layered convection is concerned.

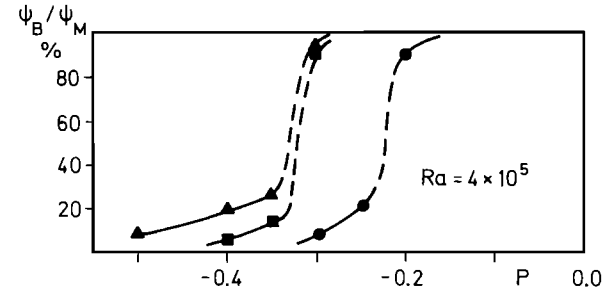

Fig. 8. Leaking rate ψ_B/ψ_M as a function of P for time-dependent convection with $Ra = 4 \times 10^5$, $Di = 0.0$. Triangles indicate results for the complete calculations, using the Γ function, and squares are results for the simulation with effective thermal expansivity, both for constant viscosity. Circles show the data for a low-viscosity zone in the transition region meant to simulate transformational superplasticity, as described in the text. The effective α' parameterization is used.

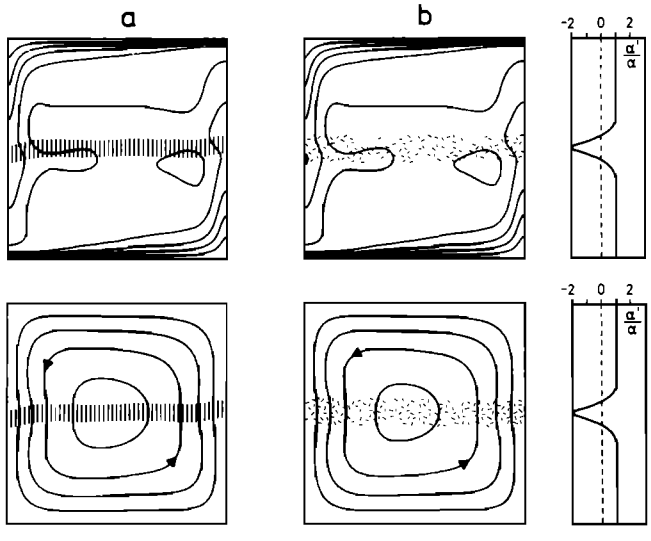

Fig. 7. Isotherms (upper diagrams) contoured at 0.1 (+0.1) 0.9 and flow lines in steps of 20 units for steady convection at $Ra = 4 \times 10^5$, $Di = 0.5$, and $P = -0.3$. (*a*) The results of the complete calculation are shown, and the region where $0.2 \leq \Gamma \leq 0.8$ is marked by vertical bars. (*b*) The equivalent model with effective expansion coefficient is shown, the area where $\alpha' < 0$ is shaded, and the depth dependence of α' is displayed to the right. The maximum stream function is 86.3 in Figure 7*a* and 83.6 in Figure 7*b*; the Nusselt number is 8.67 in Figure 7*a* and 8.60 in Figure 7*b*. The values without phase transition are $\psi_M = 104.4$ and $Nu = 6.70$, respectively.

3.3. *Effective Thermal Expansivity*

According to (19) through (21) the effect of a divariant phase transition in convection can be expressed by an effective thermal expansivity α' and an effective heat capacity c_p'. *Schubert et al.* [1975] pointed out that the effective α' can be very different from the ordinary α, while c_p' does not differ from c_p by more than a factor of 2. We tried to assess in a couple of calculations how faithfully the effect of a phase transition can be simulated by a depth-dependent, locally modified thermal expansion coefficient alone, leaving the heat capacity unchanged. Because of the deflection and the change in width of the transition region, a strictly depth-dependent α' constitutes a further simplification.

The right-hand side in the momentum equation (12) is now written as $Ra\ \alpha'/\alpha\ \partial T/\partial x$, where α' is determined from (20). In (20), $d\Gamma/d\pi$ is calculated according to (6) under the assumption that the temperature is constant ($T = 0.5$) in the transition region.

In general, we find that the effective α' simulates a phase transition almost perfectly in the single-layer regime. Figure 7 shows a comparison between the exact calculation with the Γ function and the α' representation for a non-Boussinesq case and negative P. The effective expansivity peaks at -2α. Both the positive buoyancy of the distorted phase boundary and the negative latent heat are obtained by the effective expansivity, the latter effect by the locally inverted adiabatic gradient. The flow pattern and the thermal structure are very similar to those obtained by the complete calculation.

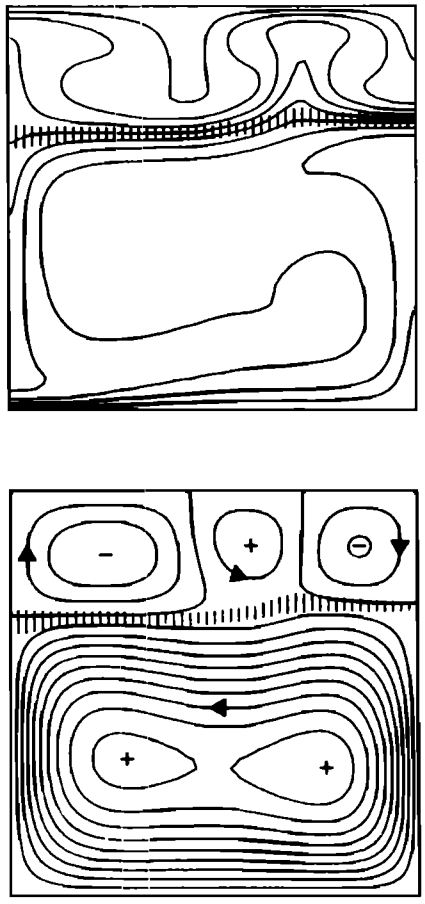

Fig. 9. Layered convection with unequal layer thickness (ratio 3:7) $Ra = 4 \times 10^5$, $Di = 0.0$, $P = -0.50$, at about 5×10^{-2} nondimensional time units. Isotherms in the upper diagram are contoured at 0.1 (+0.1) 0.9, and stream functions in the lower diagram are contoured at -10 (+5) +45.

The agreement is not quite as good in the time-dependent regime or when double-layer convection occurs. The effective α' formulation slightly underestimates the negative P which is necessary to obtain double-layer convection; e.g., with $Ra = 10^5$, $Di = 0$, and $P = -0.40$, basically single-layer convection is obtained, but the parameterization with the effective α' gives double-layer flow with a leaking rate of $\psi_B/\psi_M = 25\%$. A more extensive study at $Ra = 4 \times 10^5$ shows that the critical P is probably not more than 10% wrong, but the leaking rate predicted with the effective α' in the double-layer regime is considerably less than with the complete formulation of the phase transition problem (Figure 8). The calculations with effective α' also show a smoother temporal evolution and a less spasmodic behavior. At $Ra = 2 \times 10^6$, $P = -0.3$, now double-layer convection without episodic overturn or enhanced leaking events is obtained. The representation by a depth-dependent α' becomes exact in the limit $Rb/Ra \to \infty$, $\bar{\gamma} \to 0$ for a given value of $P = \bar{\gamma}\, Rb/Ra$. In this limit, c_p' becomes equal to c_p, and the actual geometric distortion of the transition region goes to zero. This has been verified for the above mentioned case of $Ra = 10^5$, $P = -0.4$ in a complete calculation with $Rb = 40$ Ra, $\bar{\gamma} = -0.01$. As in the effective α' representation, now double-layer convection with 25% leaking occurs.

We thus conclude that simulating a divariant phase transition by a depth-dependent effective α' is a numerically simple tool to predict its influence on convection to a reasonable degree. Furthermore, for steady single-layer convection the agreement is almost quantitatively correct.

3.4. *Superplasticity*

In order to get an idea of how transformational superplasticity affects the occurrence of layered convection, we introduce a layer of locally reduced viscosity into the transition region. We use the effective α' analogue because it leaves an undistorted transition zone in a definite depth range, which allows us to fix the viscosity once for the whole experiment. The viscosity profile is given by

$$\eta(z) = \exp\left\{-a\left[1 - \tanh^2\left(\frac{z - z_0 - \bar{\gamma}/2}{d}\right)\right]\right\} \qquad (26)$$

The parameter a is chosen so as to impose a minimum viscosity 10^{-3} times that of the viscosity outside the transition region. As may be seen in Figure 8, the transition from single- to double-layer convection at $Ra = 4 \times 10^5$ now requires a P which can be smaller by 30% in absolute value, compared with the case without superplasticity. A single result for $Ra = 2 \times 10^6$, $P = -0.20$, where double-layer convection was found with superplasticity, agrees with this conclusion.

If one regards the possibility for layered convection as depending on the degree to which the local obstructive buoyancy of the transition region can be balanced by the global driving buoyancy by viscous coupling, it is not surprising at all that superplasticity facilitates layered convection. However, we would have expected an even stronger reduction of $|P_{crit}|$ compared with what is actually found.

3.5. *Layers of Unequal Thickness*

In a last series of experiments, we tried to determine the influence of nonsymmetric layering by putting the equilibrium depth of the phase boundary to 0.7 (i.e., $\Gamma(z = 0.7, T = 0.5) = 0.5$). For the 670-km discontinuity in the earth, the ratio is 0.77 to 0.23. With constant viscosity the Rayleigh numbers of the two sublayers are no longer alike, that of the upper one being 0.014 Ra and that of the lower one being 0.17 Ra, assuming that the ΔT jumps are the same. We find that there is very little difference regarding the threshold of breakdown and the leaking rate in the double-layer regime compared with the previous cases where the transition zone was at middepth (tested for several cases at $Ra = 4 \times 10^5$ and 2×10^6). This is of importance, since it demonstrates that the results of the more comprehensive study done for equal sublayer thicknesses can be applied to the realistic case in the earth. Again, a variety of cell configurations could be obtained, including one with three cells in the upper layer (Figure 9). A systematic study on this topic, however, has not been carried out.

A stratified viscosity distribution with the higher viscosity in the lower layer seems to favor slightly the occurrence of layered convection. We took a viscosity ratio of 1 to 12.7, which makes the Rayleigh numbers of both sublayers (with a thickness ratio of 3 to 7) equal. We considered a case where the Rayleigh number of the sublayers was 2.5×10^4, the same as in the case of equal layer thickness with constant viscosity and a global $Ra = 4 \times 10^5$. While in the latter case the threshold toward layered convection was found at $P = -0.33$, we now find layered convection already at $P = -0.25$. Although we do not understand the underlying reason, this preliminary study suggests that a stratified viscosity distribution may facilitate layered convection.

4. SUMMARY AND CONCLUDING REMARKS

In our numerical experiments we have shown that an endothermic phase transition can lead to a kind of "leaky" double-layer convection. The mechanism which induces layering is the stabilizing buoyancy force connected with thermally induced phase boundary distortions. We have demonstrated that the latent heat release of the transition is a non-Boussinesq effect which scales with the dissipation number Di. Experiments with finite Di show that the latent heat effect has no influence on the point of breakdown into separately convecting layers. On the other hand, we find that the threshold for layered convection becomes smaller the higher the thermal Rayleigh number is. It is not clear what the asymptotic behavior for very high Rayleigh numbers is, but we do not expect that (25) holds for $Ra \rightarrow \infty$. Rather, we expect a finite asymptotic value for P_{crit}, which is reached when thermal expansion in the transition region itself is sufficient to overcome the buoyancy of the distorted phase boundary. In this case the effective α' would be less than α but remain positive everywhere. It depends on the thickness d of the transition zone when this point is reached.

We found the description of the phase transition by a locally modified coefficient of thermal expansion α' a convenient numerical tool which predicts the principal behavior of the system with reasonable accuracy. We would suggest using this "parameterization" by an effective α' also for other geodynamical phenomena where thermal anomalies and phase transitions play a role.

Our study gives no indication that the threshold for layered convection depends on the relative depth of the phase transition between upper and lower boundary. On the other hand, a possible viscosity reduction by transformational superplasticity would lower the threshold by about 30%. Also, a viscosity stratification could lead to a reduction of the critical P by a modest amount. However, even strong viscosity variations and non-Newtonian rheology do not seem to influence the point of breakdown into layered convection dramatically. In our previous work [*Christensen and Yuen*, 1984] we modeled a subducting slab with temperature-dependent power law rheology. In a single model series at $Ra = 8 \times 10^6$, we determined the critical phase distortion parameter P_{crit} to be in between 0.25 and 0.33 (-4.5 to -6.0 MPa/K for γ with our chosen scaling). This value agrees reasonably well with the constant viscosity results presented in this work, being perhaps slightly higher. For a chemical rather than a phase boundary we had found more pronounced differences between constant viscosity convection and cases where a lithospheric slab is an integral part of the circulation.

Extrapolating our results along the line of (25) to a Rayleigh number of $0(10^7)$, which is a likely value for whole mantle convection, and taking into account uncertainties about viscous stratification, superplasticity, or the presence of slabs, we estimate the likely range for the critical phase distortion parameter in the earth to be -0.15 to -0.30. If we scale $P = \Delta\rho\gamma/\rho^2\alpha g h$ to typical mantle values ($\Delta\rho/\rho \simeq 0.06, \cdots, 0.12$, $\rho = 4 \times 10^3$ kg m^{-3}, $\alpha = 1.5, \cdots, 2.5 \times 10^{-5}$ K^{-1}, $g = 10$ m s^{-2}, $h = 2880 \times 10^3$ m), the quoted values for P_{crit} translate into a critical Clapeyron slope approximately in the range of -4 to -8 MPa/K (-40 to -80 bar/K). This is in agreement with our previous estimate of -6 MPa/K. If the mean thermal expansivity of the mantle is rather low and transformational superplasticity in fact occurs, the critical Clapeyron slope may be as low as -4 MPa/K. The chance that the spinel $\rightarrow$ perovskite + periclase transition has such a highly negative Clapeyron slope of less than -4 MPa/K can be regarded as a remote but, nonetheless, distinct possibility.

If indeed mantle convection would be layered on grounds of an endothermic phase transition at 670 km, it is likely that the Clapeyron slope is not far from the critical value. With the high Rayleigh numbers it then appears possible that episodic breakdown of the layering or heavy leaking occurs, as we observed it at $Ra = 2 \times 10^6$ in our experiments. These episodes may be responsible for geological events like continental breakup or massive formation of new continental crust. When the Clapeyron slope is near its critical value, it also appears possible that some subducting slabs are able to penetrate below the 670-km discontinuity (Sea of Okhotsk [*Creager and Jordan*, 1984]) while others are not (Tonga [*Giardini and Woodhouse*, 1984]). Because the threshold toward layered convection increases with decreasing Rayleigh number, it also appears possible that the cooling mantle may have switched somewhere in the past from double- to single-layer convection. However, these ideas must be regarded as pure speculations at the moment. In order to determine the significance of our numerical calculations, a more careful determination of the Clapeyron slope of the spinel $\rightarrow$ perovskite + periclase transition and other candidate lower mantle transitions is needed.

Acknowledgments. We gratefully acknowledge support by the Petroleum Research Fund, administered by the American Chemical Society, under grant 13550-G2.

REFERENCES

Anderson, D. L., Phase changes in the upper mantle, *Science*, *157*, 1165–1173, 1967.

Anderson, D. L., The upper mantle transition zone: Eclogite?, *Geophys. Res. Lett.*, *6*, 433–435, 1979.

Christensen, U. R., Convection with pressure and temperature dependent non-Newtonian rheology, *Geophys. J. R. Astron. Soc.*, *77*, 343–384, 1984.

Christensen, U. R., and D. A. Yuen, The interaction of a subducting lithospheric slab with a chemical or phase boundary, *J. Geophys. Res.*, *89*, 4389–4402, 1984.

Creager, K. C., and T. H. Jordan, Slab penetration into the lower mantle, *J. Geophys. Res.*, *89*, 3031–3050, 1984.

Giardini, D., and J. H. Woodhouse, Deep seismicity and modes of deformation in Tonga subduction zone, *Nature*, *307*, 505–509, 1984.

Jackson, I., Some geophysical constraints on the chemical composition of the lower mantle, *Earth Planet. Sci. Lett.*, *62*, 91–103, 1983.

Jarvis, G. T., and D. P. McKenzie, Convection in a compressible fluid with infinite Prandtl number, *J. Fluid Mech.*, *96*, 515–583, 1980.

Jeanloz, R., and A. B. Thompson, Phase transitions and mantle discontinuities, *Rev. Geophys.*, *21*, 51–74, 1983.

Kumazawa, M., H. Sawamoto, E. Ohtani, and K. Masaki, Postspinel phase of forsterite and evolution of the mantle, *Nature*, *247*, 356–358, 1974.

Liu, L. G., Orthorhombic perovskite phases observed in olivine, pyroxene and garnet at high pressures and temperatures, *Phys. Earth Planet. Inter.*, *11*, 289–298, 1976.

Liu, L. G., On the 670 km discontinuity, *Earth Planet. Sci. Lett.*, *42*, 202–208, 1979.

McKenzie, D. P., J. M. Roberts, and N. O. Weiss, Convection in the earth's mantle: Towards a numerical simulation, *J. Fluid Mech.*, *62*, 465–538, 1974.

Olson, P., An experimental approach to thermal convection in a two-layered mantle, *J. Geophys. Res.*, *89*, 11,293–11,302, 1984.

Olson, P., and D. A. Yuen, Thermochemical plumes and mantle phase transitions, *J. Geophys. Res.*, *87*, 3993–4002, 1982.

Oxburgh, E. R., and D. L. Turcotte, Mechanisms of continental drift, *Rep. Prog. Phys.*, *41*, 1249–1312, 1978.

Richter, F. M., Finite amplitude convection through a phase boundary, *Geophys. J. R. Astron. Soc.*, *35*, 265–276, 1973.

Richter, F. M., and D. P. McKenzie, On some consequences and possible causes of layered mantle convection, *J. Geophys. Res.*, *86*, 6133–6142, 1981.

Ringwood, A. E., Phase transformations and mantle dynamics, *Earth Planet. Sci. Lett.*, *14*, 233–241, 1972.

Rubie, D. C., The olivine→ spinel transformation and the rheology of subducting lithosphere, *Nature*, *308*, 505–508, 1984.

Sammis, C. G., and J. L. Dein, On the possibility of transformational superplasticity in the earth's mantle, *J. Geophys. Res.*, *79*, 2961–2965, 1974.

Schubert, G., D. A. Yuen, and D. L. Turcotte, Role of phase transitions in a dynamic mantle, *Geophys. J. R. Astron. Soc.*, *42*, 705–735, 1975.

U. R. Christensen, Max-Planck-Institut für Chemie, Saarstrasse 23, 6500 Mainz, Federal Republic of Germany.

D. A. Yuen, Department of Geological Sciences, University of Colorado, Boulder, CO 80309.

(Received September 20, 1984;
revised April 1, 1985;
accepted May 24, 1985.)